Effects of Hindlimb Suspension on the Development of Hip Bone Morphologies in Growing Rats

Shun EZUMI[1,2], Akinori KANEGUCHI[2], Marina KANEHARA[3], Yoshitaka IWAMOTO[1,4], Makoto TAKAHASHI[1,4], Norikazu NISHIDA[3], Junya OZAWA[2]

[1]Department of Neuromechanics, Graduate School of Biomedical and Health Sciences, Hiroshima University, Hiroshima, Japan, [2]Department of Rehabilitation, Faculty of Rehabilitation, Hiroshima International University, Hiroshima, Japan, [3]Major in Medical Engineering and Technology, Graduate school of Medical Technology and Health welfare Sciences, Hiroshima International University, [4]Center for Advanced Practice and Research of Rehabilitation, Graduate School of Biomedical and Health Sciences, Hiroshima University, Hiroshima, Japan

Received June 13, 2023
Accepted March 19, 2024

Summary

Abnormal hip bone morphologies are associated with various diseases of the hip joint. Weight bearing, especially during growth, may be important to achieve normal acetabulum development. This study aimed to investigate whether hip bone morphologies were affected by hindlimb suspension (HS) in 4-week-old rats. In HS groups, tail suspension was applied for 0, 2, 4, and 8 weeks. Age-matched rats were used as controls. The complex of hip bones with lumbar and sacral vertebrae were assessed based on morphological indexes using three-dimensional reconstructed images from X-ray computed tomography. Acetabular widths (measured from cranial to caudal) unchanged and depths became larger in both groups with age. Acetabular lengths (from the ventral side to the dorsal side) became larger in control groups but unchanged in HS groups with age. In HS groups, acetabular width, length, and depths were smaller than the control groups at 4 and/or 8 weeks. Acetabular versions became enlarged (rotated inwards) with age in both groups, although this was particularly pronounced in HS groups. Histologically, triradiate cartilage layers in the acetabulum were thinner with age and almost disappeared at 8 weeks in both groups. However, HS decreased Safranin O staining and prolonged the presence of hypertrophic chondrocyte indicating alterations in the chondral ossification processes. Iliac wing angles remained unchanged and anterior superior iliac crest (ASIC) distances increased with age in controls. In contrast, HS groups showed narrowed iliac wing angles with small ASIC distances. These results suggest that reduced mechanical loading during growth can interfere with hip joint formation.

Keywords

Hindlimb suspension • Hip joint • Acetabular morphology • Triradiate cartilage

Corresponding author

Junya Ozawa, Department of Rehabilitation, Faculty of Rehabilitation, Hiroshima International University. Kurose-Gakuendai 555-36, Higashi-Hiroshima, Hiroshima, Japan. E-mail: j-ozawa@hirokoku-u.ac.jp

Introduction

Abnormal acetabulum morphologies are associated with various diseases, including osteoarthritis (OA) of the hip. In Japan, approximately 80 % of hip OA is due to acetabular dysplasia [1]. Abnormal hip joint morphology, whether subtle or obvious, can lead to pathological loading patterns that incur shear stress on the hip joint over time [2]. Therefore, inhibition of abnormal morphogenesis in the hip joint may be able to prevent the development of hip diseases.

Risk factors for hip OA include occupational heavy lifting [3], obesity [4], acetabular dysplasia [5], and pre-existing developmental dysplasia of the hip (DDH) [6]. These factors may correlate closely with mechanical stress on the hip joint. One DDH etiology is thought to be

Fax +420 241 062 164, e-mail: physres@fgu.cas.cz, www.biomed.cas.cz/physiolres

related to abnormal hip joint positioning after birth, as well as during fetal growth periods. Immobilization of newborn rat hindlimbs in extension and adduction position for ten days resulted in reduced acetabular size [7]. Therefore, bone morphogenesis is highly sensitive to mechanical stimulus, especially during the premature stage. Importantly, abnormal hip bone and/or proximal femur morphology inducing hip joint instability are considered to alter the mechanical environment within the hip joint and contribute to the development of hip OA.

Acetabular dysplasia, which can predispose individuals to hip OA [6], is characterized by reduced acetabular coverage due to a shallow socket structure [8,9]. Acetabular morphology stems from ilium, ischium, and pubic bone confluence forming the triradiate cartilage complex. Acetabulum dimensions (height, depth, and width) are determined by combined elongation on the growth plate, endochondral ossification, and additional growth [10]. Bone formation develops rapidly not only during the fetal stage and after early birth, but also following the onset of walking. Weight bearing on joints plays a pivotal role in determining femur and tibia bone morphology [11]. However, there are few studies on the effects of reduced weight loading on the hip bone except for the DDH model using neonates [7]. Especially, there are no studies evaluating the effects of hindlimb suspension during growth to our knowledge. A previous study demonstrated that distracting the triradiate cartilage complex using an external fixator in immature dogs resulted in a wider and deeper acetabulum, as well as a reduced acetabular angle [12]. Mechanical loading on the hip joint can also apply tractional stress to the triradiate cartilage complex due to its structural features. Nevertheless, the effects of reduced mechanical loading on bone morphology remains poorly understood in the acetabulum, unlike the femur and tibia [11].

Pelvic deformity, internal rotation of the hip bone, and acetabular anteversion, are common in DDH patients [9]. In addition, internal rotation of the hip bone is typically associated with decreased acetabular coverage, resulting in joint instability [9]. Theoretically, the distance between anterior superior iliac crests (ASICs) may contribute to hip bone rotation. Interestingly, there is a relationship between the degree of acetabular dysplasia and distance between anterior posterior iliac spines, an index similar to ASIC [13]. Therefore, we also focused on rotation of the hip bone and ASIC distance in this study.

We investigated the effects of weight unloading via hindlimb suspension on hip bone morphologies in 4-week-old female rats using three-dimensional (3D) computed tomography (CT) images and histological methods. Our hypotheses were as follows: 1) that acetabular length, width, and depth would decrease with early triradiate cartilage complex closure by hindlimb suspension, and 2) that acetabular version and internal rotation of hip bone would increase with suspension. Our results suggest that reduced mechanical loading during growth influences pelvic morphological development.

Methods

Experimental animals

We examined 41 premature (4-week-old) female Wistar rats purchased from Japan SLC (Shizuoka, Japan). Rats were randomly assigned to three groups: baseline (BL) group (n = 5), age-matched control (n = 6 in each subgroup), and hindlimb suspension (HS) groups (n = 6 in each subgroup). Animals in the BL group were 4 weeks old. HS and control groups were randomly assigned to three subgroups (n = 6 each) corresponding to the experimental periods of 2, 4, and 8 weeks (6, 8, and 12 weeks of age, respectively). This study was performed following approval by the Committee of Research Facilities for Laboratory Animal Sciences at Hiroshima International University.

Hindlimb suspension

Individuals in the HS groups underwent hindlimb unloading, which was performed using tail suspension method as described previously with slight modifications [14,15]. Briefly, rats were anesthetized with intraperitoneal ketamine (60 mg/kg) and xylazine (8 mg/kg) injections. One end of a piece of string was fixed to the tail using adhesive tape and the other end was attached to the top of a cylindrical cage (with a height of 36 cm and a diameter of 32 cm) *via* a swivel. Rat hindlimbs were elevated to prevent floor contact, while their forelimbs maintained contact with the floor and were allowed to move freely in the cage. In control groups, rats were housed in normal cages (3 rats per cage). All rats were housed under a 12-h light–dark cycle at room temperature of 20 – 25 °C and maintained on a diet of rodent chow and water *ad libitum*.

Tissue preparation

At the end of the experimental period, rats were weighed and killed by exsanguination under anesthesia with intraperitoneal ketamine 120 mg/kg) and xylazine (16 mg/kg) injections. Hip bones with lumbar and sacral vertebrae (spine-pelvis complex) were isolated and immersion-fixed in 0.1 M phosphate-buffered 4% para-formaldehyde (pH 7.4) for 48 h at 4ºC. After fixation, all samples were stored in phosphate-buffered saline at 4º C until X-ray CT analysis took place.

X-ray computed tomography

Spine-pelvis complexes were imaged with micro-CT (inspeXio SMX-225CT FPD HR, Shimadzu, Kyoto, Japan) at a voxel size of 37 μm (tube current: 70 μA; tube voltage: 200 KV). Bone images of the spine-pelvis complex were reconstructed from CT images using VGSTUDIO MAX software (Volume Graphics, Heidelberg, Germany). Reconstructed 3D images were converted to STL files for surface morphology analysis. We used free-form surface modeling software (Imageware9, EDS PLM Solutions, Detroit, USA) to determine landmarks and coordinate axes for quantitative morphological analyses. Acetabulum size (width, length, and depth), ASIC distance, and superior iliac angle were measured using ImageJ software (National Institutes of Health, Bethesda, USA).

Morphological analysis

Acetabular size

The measurement methods used in this study are shown in Fig. 1. Using 3D CT images, a midsagittal plane was made at the central position of the spine-pelvis complex, where both sides of the ilium were symmetrically positioned (Fig. 1–I). The nearest point to the midsagittal plane was defined as the deepest acetabulum point (Fig. 1–a). Next, the farthest point of the acetabulum along the midsagittal plane, which was the highest point of the acetabular margin, was determined at the ilium (Fig. 1–b). We then measured a plane that included the deepest acetabulum point and the highest point of the acetabular margin and was also orthogonal to the midsagittal plane (Fig. 1–II). Using this plane, the distance between acetabular margins (Fig. 1–b and c) was measured, which represented the acetabular width. We then measured a plane crossing the deepest acetabulum point orthogonal to the plane representing the acetabular width (Fig. 1–III). Using this plane, the distance between acetabular margins (Fig. 1–d and e) was measured, which denoted the acetabular length. The ratio between acetabular width and length was then expressed as an index of the circularity of the acetabulum, whereby an acetabular width/depth of 1 corresponds to a perfect circle. Acetabular depth was then measured with the plane that was used to determine the acetabular width. The distance between the deepest point and the closest point on the line connecting both acetabular margins was defined as the acetabular depth.

Acetabular version

The 3D CT images of the spine-pelvis complex were sliced in a transverse section perpendicular to the anatomical conjugate (from the promontory to the upper edge of the symphysis pubis) (Fig. 1–IV). The images used in our analyses were obtained from the central portion between the cranial and caudal sides of the acetabular margins. We then measured the angle between the line connecting the acetabular margins and the midsagittal plane (Fig. 1–θ).

Iliac wing angle

The spine-pelvis complex image was sliced into a transverse section perpendicular to the anatomical conjugate at the midpoint of the sixth lumbar vertebra (Fig. 1–V). We then measured the angle formed by medial surface tangents of the iliac wings on both sides (Fig. 1–2φ), then halved this angle to get the superior iliac angle φ.

ASIC distance

ASICs were found in slices of transverse sections of the spine-pelvis complex. Sliced images of each ASIC from the same sample were merged and the distance between left and right sides of the ASIC was measured (Fig.1–B).

Histology

Following a CT scan, hip bones were isolated from the spine-pelvis complexes. Samples were decalcified in OSTEOSOFT (Merck, Germany) for 4 weeks and embedded in paraffin. Paraffin sections (4 μm) were prepared from the acetabulum in the plane parallel to the dorsal surface of acetabular floor to measure triradiate cartilage. Sections were stained with safranin O fast green.

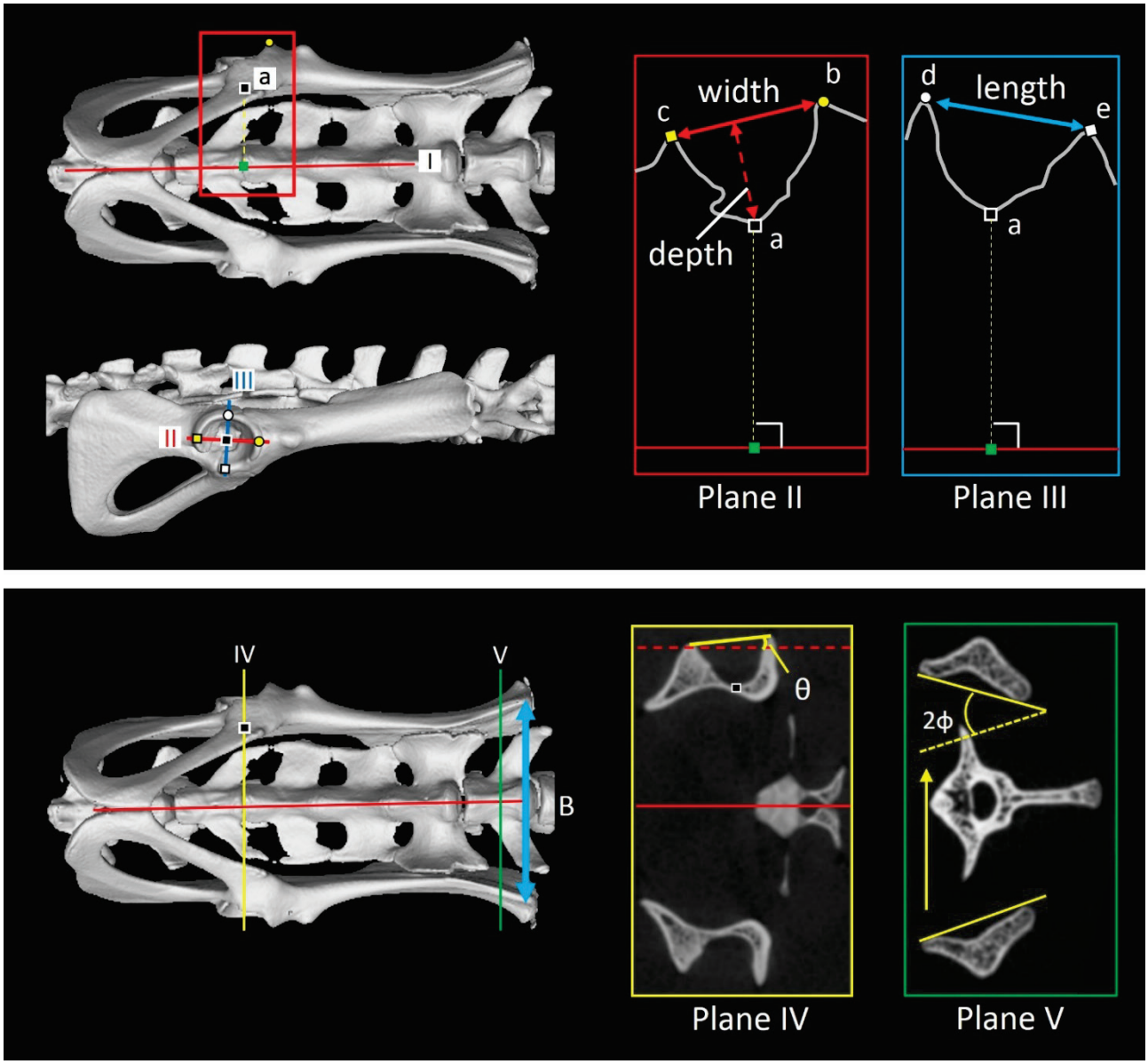

Fig. 1. Schematic representation describing how we measured morphological parameters of hip bone. The upper panel shows the way in which acetabular width, length, and depth were measured. Acetabular width: distance between points (b) and (c) on plane II. Acetabular length: distance between points (d) and (e) on plane III. Acetabular depth: distance between point (a) and the nearest point on the line connecting points (b) and (c). Plane I: a midsagittal plane at the central position of the spine-pelvis complex. Plane II: a plane sharing points (a) and (b) that is orthogonal to plane I. Plane III: a plane crossing the point (a) that is orthogonal to plane II. (a): the deepest point of the acetabulum that is the closest point to plane I. (b): the highest point on the margin of the acetabular (cranial side) that is the farthest point to plane I. (c): the point on the acetabular margin on the opposite (caudal) side of point (b) on plane II. (d): the point on the acetabular margin on the dorsal side on plane III. (e): the point on the acetabular margin on the ventral side on plane III. The lower panel shows the measured portions of the acetabular version, Iliac wing angle, and anterior superior iliac crest (ASIC) distance. Acetabular version: the angle between the line connecting the acetabular margins and plane I on plane IV (θ). Iliac wing angle: bisection of the angle formed by tangents of medial surfaces of the iliac wings on both sides (φ) on plane V. ASIC distance: distance between the left and right ASIC sides (B). Plane IV: a plane perpendicular to the line between the promontory and the centre of the dorsal aspect of the pubic symphysis that crosses point (a). Plane V: a transverse section perpendicular to the line between the promontory and the centre of the dorsal aspect of the pubic symphysis at the middle level of the sixth lumber vertebra.

Histomorphometry

The images of triradiate cartilage between the ilium and ischium were photographed using a light microscope and a digital camera (Fig. 2A, B). Images taken at 10-fold magnification were used to calculate the heights of the triradiate cartilage and hypertrophic chondrocyte zone by an image analysis software ImageJ (National Institutes of Health, Bethesda, MD, USA). The height of triradiate cartilage was defined as the mean value of cartilage length between the upper and lower mineralized tissues. The hypertrophic zone was defined the mean value of length from the first chondrocyte with

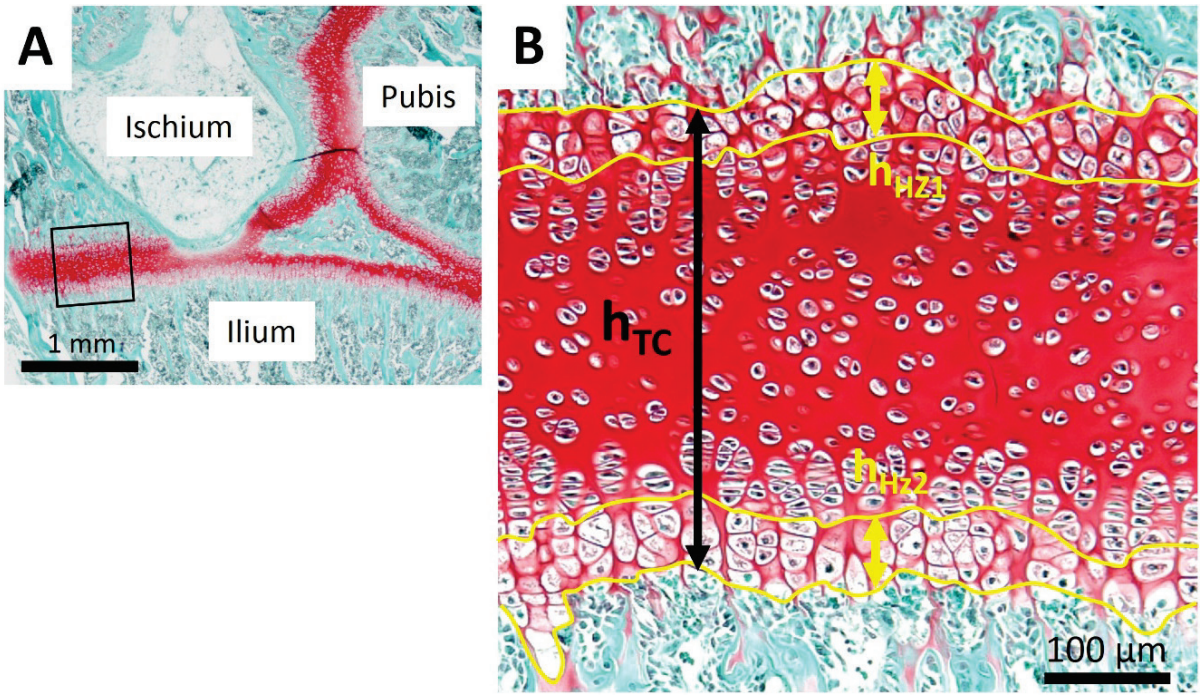

Fig. 2. Light micrographs of triradiate cartilage illustrating the histomorphometric measurements. (**A**) Histological section in the plane parallel to the dorsal surface of acetabular floor stained with Safranin O fast green was used to analyze the triradiate cartilage. (**B**) The triradiate cartilage between the ischium-ilium, enlarged and boxed in A. h_{TC}: Height of the triradiate cartilage. h_{Hz1}: Height of the hypertrophic zone of the ischium side. h_{Hz2}: Height of the hypertrophic zone of the ilium side. The height of hypertrophic zone was calculated as $h_{HZ1} + h_{HZ2}$.

markedly enlarged volume compared to proliferating cells to the border of mineralized tissue. The height of hypertrophic zone was calculated on both ilium and ischium sides and summed to obtain the total hypertrophic zone. The height of triradiate cartilage at 8 weeks and the height of hypertrophic zone at 4 and 8 weeks in both groups were not measured because they could not be clearly distinguished or observed.

Statistics

All data were expressed as means ± standard deviation (SD). Statistical analyses were performed using SPSS for Windows (IBM SPSS Statistics ver. 28.0, Tokyo, Japan). We applied two-way analysis of variance (ANOVA) for all parameters except the hypertrophic zone to examine the relationship between intervention (HS) and experimental period (age in weeks). If significant interaction or direct effects were detected, we performed post-hoc Bonferroni tests to localize the effects. For the hypertrophic zone, non-parametric Kruskal-Wallis test followed by Bonferroni's post hoc test was performed to detect significant differences among three groups (BL, control, and HS at 2 weeks). For all tests, a P-value of less than 0.05 was considered statistically significant.

Results

Body weights, acetabular morphologies, iliac wing angles, and ASIC distances are shown in Table 1.

Body weights

Body weights were significantly higher with age among both controls (BL vs. 2w; 2w vs. 4w; 4w vs. 8w; all $P < 0.001$) and HS groups (BL vs. 4w, $P < 0.001$; 4w vs. 8w, $P < 0.001$). Compared with age-matched controls, HS groups were lower at any time point (all $P < 0.05$). We found a significant interaction between HS and age. We also detected main effects for both HS and age.

Acetabular morphology

Acetabular morphologies are shown in Table 1. In acetabular widths, we found no difference among both controls and HS groups during the experimental period. When comparing the two groups, acetabular widths in the HS group trended to be higher than the control group at 2 weeks ($P = 0.067$) and was significantly higher at 4 weeks ($P = 0.017$). There was a significant main effect for HS. We found no significant interaction effect between HS and age and no main effect for age.

Acetabular lengths in the control groups were longer with age (BL vs. 4w, P = 0.003; BL vs. 8w, P = 0.001). In contrast, we found no difference in acetabular lengths among HS groups. When comparing the two groups, acetabular lengths in the HS groups were significantly longer than the control groups at 4 and 8 weeks (P = 0.045 and P = 0.028, respectively). There were significant main effects for both HS and age. We found no significant interaction effect between HS and age.

Acetabular depths were larger with age among both control (BL vs. 2w, P < 0.001; BL vs. 4w, P < 0.001; BL vs. 8w, P < 0.001; 2w vs. 8w, P = 0.036) and HS groups (BL vs. 4w, P < 0.001; BL vs. 8w, P < 0.001; 2w vs. 8w, P = 0.035). When comparing the two groups, acetabular depths in the HS groups were significantly smaller than the control groups at 2 and 8 weeks (P = 0.016 and P = 0.009, respectively). There were significant main effects for both HS and age. We found no significant interaction effect between HS and age.

Acetabular version angles were larger with age among both controls (BL vs. 2w, P = 0.004; BL vs. 4w, P = 0.003; BL vs. 8w, P = 0.029) and HS groups (BL vs. 2w; BL vs. 4w; BL vs. 8w, all P < 0.001). When comparing the two groups, acetabular version angles in the HS groups were significantly larger than the control groups at 2, 4, and 8 weeks (P = 0.002, P = 0.001, and P = 0.001, respectively). There were significant main effects for both HS and age. We found no significant interaction effect between HS and age.

Table 1. Body weight, acetabular morphologies, iliac wing angle, and ASIC distance

		Experimentral periods				Two-way ANOVA (*P*-values)		
	Group	BL (0w)	2w	4w	8w	Interaction	Main effect HS	Main effect age
Body weight (g)	Control	85 ± 5^{a}	124 ± 6^{b}	150 ± 7^{c}	181 ± 10^{d}	**0.007**	**< 0.001**	**< 0.001**
	HS		98 ± 11^{a}*	124 ± 16^{b}*	154 ± 12^{c}*			
Acetabular morphologies								
Width (mm)	Control	4.39 ± 0.10^{a}	4.33 ± 0.13^{a}	4.39 ± 0.06^{a}	4.31 ± 0.18^{a}	0.365	**0.007**	0.840
	HS		4.18 ± 0.20^{a}	4.20 ± 0.12^{a}*	4.21 ± 0.07^{a}			
Length (mm)	Control	3.84 ± 0.14^{a}	3.97 ± 0.04^{ab}	4.11 ± 0.09^{b}	4.12 ± 0.10^{b}	0.413	**0.005**	**< 0.001**
	HS		3.86 ± 0.11^{a}	3.96 ± 0.14^{a}*	3.97 ± 0.12^{a}*			
Depth (mm)	Control	2.46 ± 0.02^{a}	2.74 ± 0.06^{b}	2.81 ± 0.10^{bc}	2.91 ± 0.11^{c}	0.238	**0.003**	**< 0.001**
	HS		2.59 ± 0.14^{ab}	2.73 ± 0.15^{bc}*	2.76 ± 0.09^{c}*			
Version angle (°)	Control	4.7 ± 1.8^{a}	8.7 ± 2.2^{b}	8.6 ± 1.4^{b}	7.7 ± 1.3^{b}	0.058	**< 0.001**	**< 0.001**
	HS		12.4 ± 1.3^{b}*	12.4 ± 1.7^{b}*	11.4 ± 2.5^{b}*			
Iliac wing angle (°)								
	Control	12.3 ± 0.8^{a}	12.8 ± 1.2^{a}	10.1 ± 3.0^{a}	11.3 ± 4.6^{a}	0.115	**0.002**	**0.028**
	HS		7.2 ± 3.6^{b}*	8.2 ± 2.0^{ab}	6.2 ± 4.8^{b}*			
ASIC distance (mm)								
	Control	10.0 ± 0.3^{a}	11.8 ± 0.4^{b}	12.6 ± 0.6^{b}	14.5 ± 0.7^{b}	0.084	**0.002**	**< 0.001**
	HS		10.5 ± 0.3^{ab}*	11.7 ± 0.7^{b}	13.7 ± 1.3^{c}			

Different letters indicate statistically significant differences among HS or control groups (P < 0.05). * indicates the values in the HS group were significantly different (P < 0.05). Cont, contralateral side; Immo, immobilized side. Values are mean ± standard deviation. Note: Statistically significant values for two-way ANOVA are indicated in bold.

Iliac wing angle

In iliac wing angles, we found no difference among control groups during the experimental period. In contrast, iliac wing angles were smaller with age among HS groups (BL vs. 2w, P = 0.025; BL vs. 8w, P = 0.024). When comparing the two groups, iliac wing angles in the HS groups were significantly smaller than the control groups at 2 and 8 weeks (P = 0.002 and P = 0.013,

respectively). We found no significant interaction effect between HS and age. There were significant main effects for both HS and age.

ASIC distance

ASIC distances were larger with age among both controls (BL vs. 2w, $P < 0.001$; BL vs. 4w, $P < 0.001$; BL vs. 8w, $P < 0.001$; 2w vs. 8w, $P = 0.002$) and HS groups (BL vs. 4w, $P = 0.010$; BL vs. 8w, $P < 0.001$; 4w vs. 8w, $P = 0.001$). When comparing the two groups, ASIC distances in the HS group were significantly smaller than the control groups at 2 weeks ($P < 0.001$). There was a significant main effect for both HS and age. No significant interaction effect between HS and age was found.

Triradiate cartilage histology

Fig. 3 shows histological sections from the triradiate cartilage between the ilium and ischium. Triradiate cartilages stained with safranin O were the thickest at BL and became thinner with age in both groups (Figs. 3A-G). Histomorphometric analysis also showed that the heights of triradiate cartilage were significantly smaller with age in both the control (BL vs. 2w, $P = 0.006$; 2w vs. 4w, $P = 0.006$) and HS groups (BL vs. 2w, $P = 0.008$; BL vs. 4w, $P < 0.001$) (Fig. 4A). When comparing the two groups, there were no differences at any time point. There was a significant main effect for age ($P < 0.001$). No significant interaction effect between HS and age ($P = 0.714$) and no main effect for HS ($P = 0.521$) were found. Staining intensity of safranin O hardly varied with age in the control groups, but appeared to decrease in the HS groups at 2 and 4 weeks compared to the age-matched controls (Figs. 3B, C, E, F). At 8 weeks, hyaline cartilage was slightly stained, but the layers almost disappeared in both groups (Figs. 3D, G).

Chondrocytes in proliferating and maturation /hypertrophic states were clearly observed in BL group (Fig. 3H). At 2 weeks, hypertrophic chondrocyte layers in the HS group were clearly seen (Fig. 3K), whereas hypertrophic chondrocytes were scarce in the control (Fig. 3I). At 4 weeks, hypertrophic chondrocytes were practically absent and mature chondrocytes were

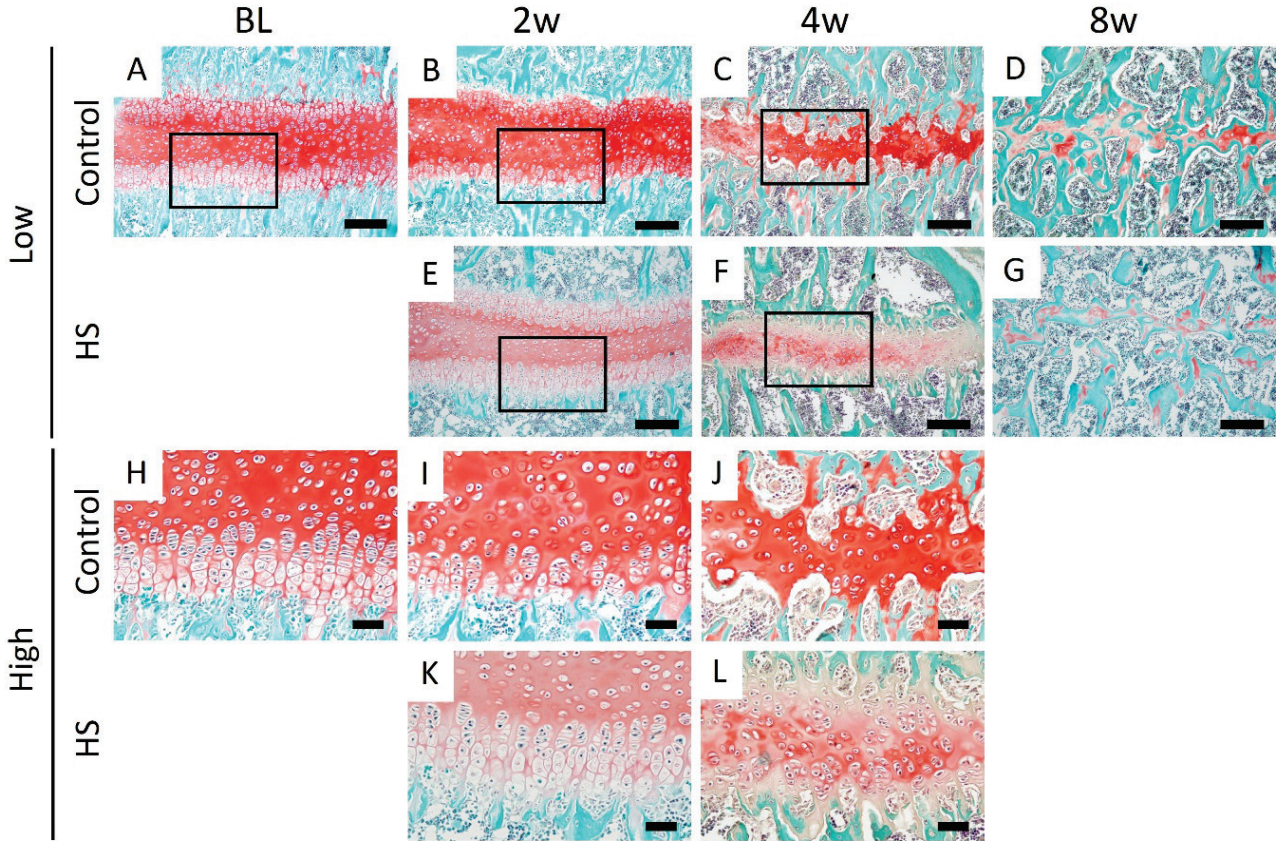

Fig. 3. Histological changes in the triradiate cartilage of hip bones. Representative images of triradiate cartilage stained with safranin O at baseline (A and H), 2 weeks (B, E, I, K), 4 weeks (C, F, J, L), and 8 weeks (D and G) of hindlimb suspension (E, F, G, K, L) and age-matched controls (B, C, D, I, and J). Higher magnification of squared areas in A, B, C, E, and F (upper section) are shown in H, I, J, K, and L, respectively (lower section). Scale bars are 200 μm in A–G and 50 μm in H–L.

scattered in the control group (Fig. 3J). In the HS groups, however, enlarged chondrocytes still exist (Fig. 3L). Histomorphometric analysis showed that the heights of hypertrophic zone were significantly smaller in the control at 2 weeks than BL ($P < 0.007$) (Fig. 4B). In the HS group, however, the height of hypertrophic zone was comparable to the BL level ($P = 0.730$) as well as age-matched control ($P = 0.255$).

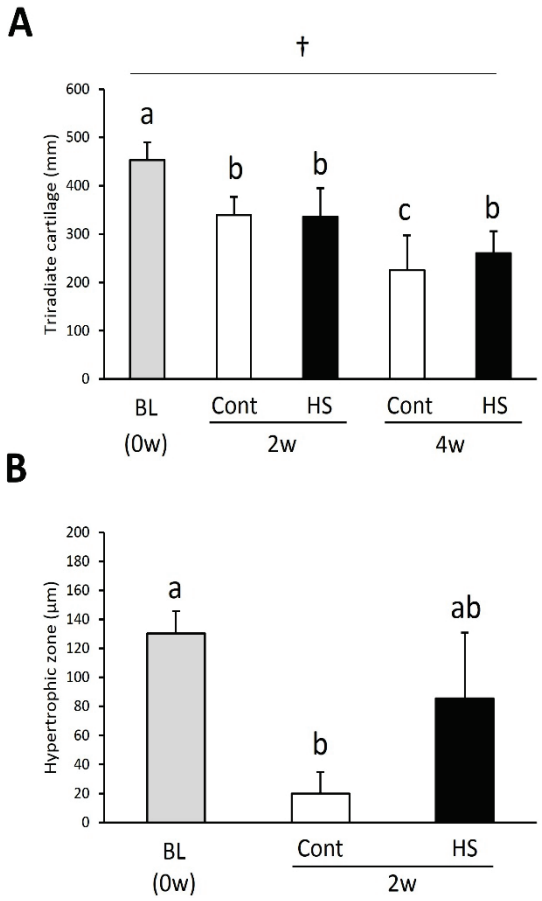

Fig. 4. Histomorphometric analysis of the triradiate cartilage. (**A**) Height of the triradiate cartilage. (**B**) Height of the hypertrophic zone. † indicates a significant main effect for age ($P < 0.05$). Different letters (a, b, and c) indicate statistically significant differences among HS or control groups ($P < 0.05$). Values are mean ± standard deviation. BL, baseline; Cont, control; HS, hindlimb suspension.

Discussion

This study investigated the effects of hindlimb suspension on the morphogenesis of hip bones in growing rats. In HS rats, acetabular size was smaller, acetabular version increased than control groups. Triradiate cartilage was thinner and proteoglycan content decreased at 2 and 4 weeks in HS groups. The hypertrophic chondrocytes zone remained larger, indicating delayed chondral ossification processes. Iliac wing angles and ASIC distances decreased following hindlimb suspension. Our study shows that reduced mechanical stress affects formation of hip bone morphologies even after locomotion onset.

Acetabular lengths (measured from the ventral side to the dorsal side) increased between 4- and 12-week-old rats in control groups, suggesting length may vary within this period. Conversely, acetabular width (measured from the cranial side to the caudal side) did not change significantly during the experimental period in either group. These results indicate acetabulum growth processes in terms of width and length vary depending on direction, and that acetabular width may stop growing earlier than length. Moreover, acetabular width/length ratios, an index for acetabulum circularity, were smaller (indicating increased circularity) with growth in control groups, but not HS groups. Ground reaction force is considered to be an input to the acetabulum from the ventral to caudal direction via the femoral head during quadrupedal locomotion in rats. Leg bone architecture is stimulated by micro- or hypergravity [11,16] and running [17]. In addition, we found that reduced mechanical stress caused by hindlimb unloading stopped acetabular length extension during growth. These results may explain the crucial role played by weight bearing in the formation of acetabular margin shape.

Acetabular depths increased with age in both groups, however, we detected significant differences between groups at 4 and 8 weeks, indicating that acetabular depths were smaller in HS groups than age-matched controls. Several studies report that experimentally-induced abnormal mechanical environments facilitate dysplastic changes in hip joints [7,18]. For instance, one study found that acetabular length, width, and depth in newborn DDH model rats that were placed into a straight-leg swaddling position were smaller than age-matched controls [7]. Ford *et al.* [19] reported the effects of reduced mechanical stress on hip joints *via* intramuscular injection of botulinum toxin in newborn rats: they found that botulinum toxin injection reduced acetabular coverage of the femoral head and caused morphological shape changes in the hip. Our present study shows that hindlimb suspension can induce dysplastic changes in the acetabulum not only in newborn rats, but also in rats that have completed locomotion skill acquisition.

We determined that acetabular sizes were smaller in HS groups. Acetabular development is

attributed to the confluence of the ilium, ischium, and pubic bones, which make up the triradiate cartilage complex [10,20]. In addition, one study found that acetabular sizes decreased when eliminating mechanical stress after hindlimb amputation or femoral head excision in newborn rats [21]. Therefore, we speculated that hypoplastic acetabulum induced by hindlimb suspension may be due to early closure of the triradiate cartilage complex. Unexpectedly, there was no apparent difference in the timing of triradiate cartilage complex closure between the two groups, according to histological observations. On the other hand, safranin O staining decreased at 2 and 4 weeks in HS groups, which indicates lower proteoglycan content. In addition, hindlimb unloading disturbed the chondral ossification process in the triradiate cartilage. Specifically, the hypertrophic layers remained in the HS group at 2 weeks, although these were rarely observed in the age-matched control group. This result may indicate delayed differentiation processes in chondrocytes, which translates to delayed replacement of cartilage replacement with bone. Furthermore, inhibition of acetabular growth may at least in part be explained by delayed ossification in the triradiate cartilage. Previous reports show that the mechanical environment influences cartilage differentiation in the growth plate [22]. This study showed that increased mechanical stress due to running exercise, contrary to our experimental setting, decreases hypertrophic zone in the rat femur.

In a previous study, acetabular anteversion increased during pre- and post-closure of the triradiate cartilage complex in humans [23]. Therefore, we speculated that acetabular version increases with growth. We revealed that the acetabular version angle in control groups increased with growth in accordance with a previous study. However, we detected a significant difference in angle between BL (4-week-old) and 2 weeks (6-week-old), which is the time before closure of the triradiate cartilage complex (from 8- to 12-week-old rats). The reason why these results differed from human results in the previous study is unknown. In addition, hindlimb suspension promoted acetabular anteversion with age. Furthermore, acetabular version is influenced by morphologic features of the entire pelvis. Fujii *et al.* [9] reported that internal rotation of the hip bone is associated with an increased acetabular anteversion angle. In this study, iliac wing angles were smaller in HS groups, compared to control groups. Therefore, acetabular anteversion in the HS group can be explained by internal rotation of the hip bone expressed, at least in part, as a reduced iliac wing angle. Importantly, internal rotation of the hip bone and acetabular anteversion are pronounced in patients with DDH compared with controls [9].

Mechanical loading plays an important role in bone formation through osteoblasts. Mechanical strain regulates osteogenesis via signaling pathways such as alphavbeta3-integrin [24], extracellular signal-regulated kinase (ERK1/2), and Wnt/b-catenin [25]. *In vitro* studies, mechanical stretch promotes proliferation, cell viability, and decreased the activities of apoptosis in human osteoblasts [26]. On the other hand, the impact of compression stress on the proliferation of osteoblasts or bone formation is controversial. During weight loading, the acetabulum would be subjected to both compression stress from the femoral head and stretch tension at the interface between the triradiate cartilage and the three hip bones. Thus, the decreased size and changed shape in acetabulum after HS may be due to inhibition of bone remodeling via osteoblast dysfunction.

Our study showed that body weights increased with age in both groups, but rats in HS groups were lighter than the control groups. We previously reported that hindlimb suspension induces a significant decrease in wet weights of various lower extremity muscles [15]. Therefore, inhibition of weight gain in HS groups may be partially explained by atrophy of lower extremity muscles. Hip muscle dysfunction induced by Botulinum toxin injection inhibits the growth of acetabulum and femoral head. In addition, the triradiate cartilage on the side injected with Botulinum toxin was thinner on the contralateral side [19]. Thus, hip muscle atrophy following hindlimb suspension also can be another factor for the morphological changes in hip bone.

Limitations

There are several limitations to this study. First, notable differences in the mechanical environment in hip joints exist between rat quadrupedal and human bipedal mobility. Therefore, the results of this study cannot be generally applied to humans. However, it is important to note that quadrupedal locomotion precedes bipedal locomotion in human motor skill development [27]. Second, we found abnormal morphologies associated with hip OA in unloaded growing rat hip joints. However, it is unclear whether reduced mechanical

loading will actually induce pathological changes, such as hip OA, in the future. Third, histomorphometric analysis of triradiate cartilage was limited to only between the ischium and ilium and was not not performed between the ilium and pubis or ischium and pubis.

Conflict of Interest

There is no conflict of interest.

Acknowledgements

This study was supported by the Japan Society for the Promotion of Science (KAKENHI Grant no. 21H03346).

References

1. Jingushi S, Ohfuji S, Sofue M, Hirota Y, Itoman M, Matsumoto T, Hamada Y *et al.* Multiinstitutional epidemiological study regarding osteoarthritis of the hip in japan. J Orthop Sci 2010;15:626-631. https://doi.org/10.1007/s00776-010-1507-8
2. Sandell LJ. Etiology of osteoarthritis: Genetics and synovial joint development. Nat Rev Rheumatol 2012;8:77-89. https://doi.org/10.1038/nrrheum.2011.199
3. Yoshimura N, Sasaki S, Iwasaki K, Danjoh S, Kinoshita H, Yasuda T, Tamaki T *et al.* Occupational lifting is associated with hip osteoarthritis: A japanese case-control study. J Rheumatol 2000;27:434-440.
4. Wang Y, Simpson JA, Wluka AE, Teichtahl AJ, English DR, Giles GG, Graves S *et al.* Relationship between body adiposity measures and risk of primary knee and hip replacement for osteoarthritis: A prospective cohort study. Arthritis Res Ther 2009;11:R31. https://doi.org/10.1186/ar2636
5. Gala L, Clohisy JC, Beaule PE. Hip dysplasia in the young adult. J Bone Joint Surg Am 2016;98:63-73. https://doi.org/10.2106/JBJS.O.00109
6. Harris WH. Etiology of osteoarthritis of the hip. Clin Orthop Relat Res 1986:20-33. https://doi.org/10.1097/00003086-198612000-00004
7. Bo N, Peng W, Xinghong P, Ma R. Early cartilage degeneration in a rat experimental model of developmental dysplasia of the hip. Connect Tissue Res 2012;53:513-520. https://doi.org/10.3109/03008207.2012.700346
8. Harris JD, Lewis BD, Park KJ. Hip dysplasia. Clin Sports Med 2021;40:271-288. https://doi.org/10.1016/j.csm.2020.11.004
9. Fujii M, Nakashima Y, Sato T, Akiyama M, Iwamoto Y. Pelvic deformity influences acetabular version and coverage in hip dysplasia. Clin Orthop Relat Res 2011;469:1735-1742. https://doi.org/10.1007/s11999-010-1746-1
10. Ponseti IV. Growth and development of the acetabulum in the normal child. Anatomical, histological, and roentgenographic studies. J Bone Joint Surg Am 1978;60:575-585. https://doi.org/10.2106/00004623-197860050-00001
11. Ohira Y, Kawano F, Wang XD, Sudoh M, Iwashita Y, Majima HJ, Nonaka I. Irreversible morphological changes in leg bone following chronic gravitational unloading of growing rats. Life Sci 2006;79:686-694. https://doi.org/10.1016/j.lfs.2006.02.022
12. Akbas A, Unsaldi T, Koruklu O, Goze F. The effect of physeal traction applied to the triradiate cartilage on acetabular growth. Int Orthop 1995;19:122-126. https://doi.org/10.1007/BF00179973
13. Okano K, Jingushi S, Ohfuji S, Sofue M, Hirota Y, Itoman M, Hamada Y *et al.* Relationship of acetabular dysplasia in females with osteoarthritis of the hip to the distance between both anterior superior iliac spines. Med Sci Monit 2014;20:116-122. https://doi.org/10.12659/MSM.889704
14. Kaneguchi A, Ozawa J, Kawamata S, Kurose T, Yamaoka K. Intermittent whole-body vibration attenuates a reduction in the number of the capillaries in unloaded rat skeletal muscle. BMC Musculoskelet Disord 2014;15:315. https://doi.org/10.1186/1471-2474-15-315
15. Ozawa J, Kaneguchi A, Ezumi S, Maeno T, Iwazawa J, Minanimoto K, Ikeda A. Effects of hindlimb suspension on development of proximal and distal femur morphological abnormalities in growing rats. J Orthop Res 2022. https://doi.org/10.1002/jor.25352
16. Canciani B, Ruggiu A, Giuliani A, Panetta D, Marozzi K, Tripodi M, Salvadori PA *et al.* Effects of long time exposure to simulated micro- and hypergravity on skeletal architecture. J Mech Behav Biomed Mater 2015;51:1-12. https://doi.org/10.1016/j.jmbbm.2015.06.014

17. Hamann N, Kohler T, Muller R, Bruggemann GP, Niehoff A. The effect of level and downhill running on cortical and trabecular bone in growing rats. Calcif Tissue Int 2012;90:429-437. https://doi.org/10.1007/s00223-012-9593-
18. Wang E, Liu T, Li J, Edmonds EW, Zhao Q, Zhang L, Zhao X *et al.* Does swaddling influence developmental dysplasia of the hip?: An experimental study of the traditional straight-leg swaddling model in neonatal rats. J Bone Joint Surg Am 2012;94:1071-1077. https://doi.org/10.2106/JBJS.K.00720
19. Ford CA, Nowlan NC, Thomopoulos S, Killian ML. Effects of imbalanced muscle loading on hip joint development and maturation. J Orthop Res 2017;35:1128-1136. https://doi.org/10.1002/jor.23361
20. Dong Y, Wang J, Qin J, Nan G, Su Y, He B, Cai W *et al.* Retrospective analysis of traumatic triradiate cartilage injury in children. BMC Musculoskelet Disord 2021;22:674. https://doi.org/10.1186/s12891-021-04565-2
21. Harrison TJ. The influence of the femoral head on pelvic growth and acetabular form in the rat. J Anat 1961;95:12-24.
22. Niehoff A, Kersting UG, Zaucke F, Morlock MM, Bruggemann GP. Adaptation of mechanical, morphological, and biochemical properties of the rat growth plate to dose-dependent voluntary exercise. Bone 2004;35:899-908. https://doi.org/10.1016/j.bone.2004.06.006
23. Albers CE, Schwarz A, Hanke MS, Kienle KP, Werlen S, Siebenrock KA. Acetabular version increases after closure of the triradiate cartilage complex. Clin Orthop Relat Res 2017;475:983-994. https://doi.org/10.1007/s11999-016-5048-0
24. Wozniak M, Fausto A, Carron CP, Meyer DM, Hruska, KA. Mechanically strained cells of the osteoblast lineage organize their extracellular matrix through unique sites of alphavbeta3-integrin expression. J Bone Miner Res 2000;15:1731-1745. https://doi.org/10.1359/jbmr.2000.15.9.1731
25. Motie P, Mohaghegh S, Kouhestani F, Motamedian SR. Effect of mechanical forces on the behavior of osteoblasts: a systematic review of in vitro studies. Dent Med Probl 2023;60:673-686. https://doi.org/10.17219/dmp/151639
26. Zhang J, Xu S, Zhang Y, Zou S, Li X. Effects of equibiaxial mechanical stretch on extracellular matrix-related gene expression in human calvarial osteoblasts. Eur J Oral Sci 2019; 127:10-18. https://doi.org/10.1111/eos.12595
27. Winders P, Wolter-Warmerdam K, Hickey F. A schedule of gross motor development for children with down syndrome. J Intellect Disabil Res 2019;63:346-356. https://doi.org/10.1111/jir.12580